Comparison of CO production and Escherichia coli inactivation by a kHz and a MHz plasma jet

Eloïse Mestre, Inna Orel, Daniel Henze, Laura Chauvet, Sebastian Burhenn, Sébastien Dozias, Fabienne Brulé-Morabito, Judith Golda, Claire Douat

Received: 25 September 2023 | Revised: 15 November 2023 | Accepted: 4 December 2023

DOI: 10.1002/ppap.202300182

PLASMA PROCESSES AND POLYMERS

RESEARCH ARTICLE

Comparison of CO production and *Escherichia coli* inactivation by a kHz and a MHz plasma jet

Eloïse Mestre[1] | **Inna Orel**[1] | **Daniel Henze**[2] | **Laura Chauvet**[2] | **Sebastian Burhenn**[2] | **Sébastien Dozias**[1] | **Fabienne Brulé-Morabito**[3] | **Judith Golda**[2] | **Claire Douat**[1]

[1]GREMI UMR7344 CNRS, Université d'Orléans, Orléans, France

[2]Plasma Interface Physics, Ruhr University Bochum, Bochum, Germany

[3]Centre de Biophysique Moléculaire (CBM), CNRS UPR 4301, Orléans, France

Correspondence
Claire Douat, GREMI UMR7344 CNRS, Université d'Orléans, Orléans France.
Email: claire.douat@univ-orleans.fr

Funding information
Deutscher Akademischer Austauschdienst France; Deutsche Forschungsgemeinschaft; French program PHC Procope, Grant/Award Number: 48122NF; French Research Agency, ANR, Grant/Award Number: MediCO-Plasma|ANR-21-CE19-0005

Abstract

As carbon monoxide has a broad spectrum of biological activities, its production by plasma is a significant advantage in medicine. This paper presents a comparative study of the CO production of two plasma jets: a MHz-jet and a kHz-jet. Both were fed with a helium gas with CO_2 admixture (0%–1%). CO was produced by CO_2 dissociation and its maximal concentration was hundreds of parts per million, which is safe for clinical applications. For the same specific energy input, the CO production was more efficient for the kHz-jet than the MHz-jet. Both had antibacterial properties on *Escherichia coli*, and the addition of CO_2 improved them for the MHz-jet, while it reduced them for the kHz-jet.

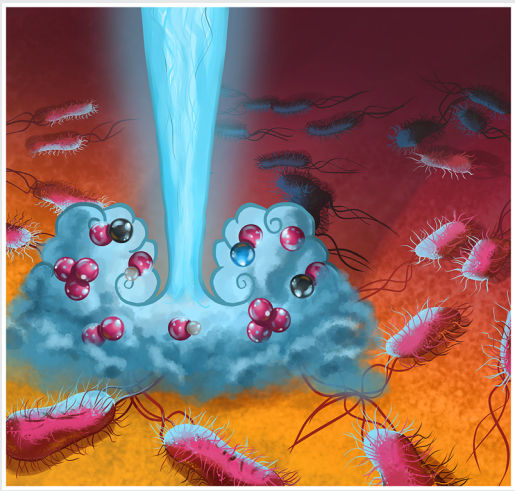

KEYWORDS
carbon monoxide (CO), CO_2 conversion, plasma jet, plasma medicine

1 | INTRODUCTION

Nonequilibrium atmospheric-pressure plasmas have drawn a growing interest in low-temperature plasma research over the last two decades, which has led to the development of a large variety of plasma sources.[1] They combine the advantage of creating a wide range of reactive species with radiation and potentially electric field while maintaining the gas temperature near room temperature. Thus, they are being investigated in various fields such as food preservation, agriculture, and medicine.[2]

In contact with living tissue, nonequilibrium atmospheric-pressure plasmas have various beneficial effects, including antibacterial, vasodilatory, antiapoptotic, anticancer, and antiproliferative effects, making them interesting for the fields of oncology, dermatology, and wound

healing.[3] However, the role of plasma in inflammation regulation remains unclear. Some studies on animals and humans show that plasma has no effect on the inflammation stage, while other studies show that it has a proinflammatory or an anti-inflammatory effect.[4] In the literature, nitric oxide (NO) is often cited as a potential molecule responsible for inflammation regulation in plasma treatment due to its important role in wound healing.[5,6] It is responsible for both the upregulation and the downregulation of the inflammatory phase and acts as proinflammatory or anti-inflammatory depending on its concentration.[5] As NO is a highly reactive species, controlling the number of molecules on the target by plasma is a big challenge, especially in the context of inflammation regulation.

In this context, this paper proposes to use plasma for producing carbon monoxide (CO). Although this molecule has a bad reputation due to the potentially lethal consequences when inhaled at high concentrations, at low concentrations, it has a broad spectrum of biological activities such as anti-inflammatory, vasodilatory, anti-apoptotic, and antiproliferative effects.[7] Moreover, this molecule is stable and less reactive than NO and may offer the advantage of better control of its delivery to the target.[8,9] Unlike NO, CO is always anti-inflammatory and does not have a proinflammatory effect when varying its concentration.[8]

The storage of CO is often classified as hazardous in health institutes. One way around this issue is the direct production of CO assisted by plasma via CO_2 dissociation.[9–12] This process has been explored with plasma jets driven by excitation frequencies ranging from kHz to MHz.[13–15] However, a kHz excitation exhibits a very different plasma from an MHz excitation. For the kHz case, at each cycle, a breakdown occurs and induces a plasma ignition. Whereas for the MHz case, there is only one breakdown and the plasma does not extinguish between two successive cycles. This is mainly due to the fact that the recombination time exceeds the period time of MHz excitation. Additionally, due to the electrode geometry, the plume is an afterglow with MHz excitation, while it is an active plasma with kHz excitation. No direct comparison of these plasma jet variations using kHz and MHz excitation has been investigated to produce CO by CO_2 dissociation in a helium plasma jet, and to fill this gap, this paper proposes a comparative study of these two plasma jet variations with fixed input parameters such as the gas flow, the gas composition, and the specific energy input (SEI).

Two different kinds of discharges were studied: a sinusoidal MHz discharge provided by the European Cooperation for Science and Technology (COST) plasma jet[16] and a kHz pulsed discharge provided by a coplanar–coaxial dielectric barrier discharge (DBD) plasma jet. The excitation frequency can have an impact on CO_2 dissociation[9,17] and will be explored in the present paper. Especially in the context of plasma medicine, these two jets represent complementary configurations: the MHz-jet is an indirect plasma source providing plasma-produced radicals only, whereas the kHz-jet also provides charged species and radicals produced in the plasma plume.

Plasma jet fed with argon or helium with and without the addition of molecular gas in the gas mixture has demonstrated its ability to inactivate bacteria.[2,18–21] But as far as we know, the use of CO_2 in the gas mixture has never been explored to evaluate the antibacterial properties of plasma in these conditions. CO_2 has no antibacterial property while the effect of CO on bacteria remains unclear. Currently, the scope of the literature on that topic is too small to have a clear idea of the potential antibacterial properties of CO molecules.[22,23] CO may hinder the activity of macrophages and thus influence bacteria inactivation,[22] while Desmard et al. demonstrated *in vitro* that CO-releasing molecules exert a significant bactericidal effect with *Pseudomonas aeruginosa*.[24] Louise Wilson et al. demonstrated that saturated CO gas solution had little effect on the inhibition of bacterial growth for both *Staphylococcus aureus* and *Escherichia coli* bacteria, whereas CO-releasing molecules with a concentration much lower than the saturated concentration of CO showed efficient antibacterial activity.[23,25] The interpretation of this result is complicated, but it shows that the CO detailed antibacterial mechanism needs to be further investigated.

In this paper, we will evaluate the antibacterial properties of the two plasma jets with and without the addition of CO_2 in the gas mixture. The impact of CO molecules on the bacteria will be investigated and compared.

2 | EXPERIMENTAL SETUP

2.1 | The kHz- and MHz-jet reactors

In this study, we used two different plasma jets with different excitation frequencies: a pulsed kHz plasma jet, hereafter called *kHz-jet*, and an AC MHz excitation plasma jet, hereafter called *MHz-jet*. The schemes and the pictures of these two jets are shown in Figure 1: (a) and (c) for the MHz-jet; (b) and (d) for the kHz-jet. Different parameters and specificity of the two jets are briefly summarized in Table 1.

The MHz-jet (Figure 1a) was composed of two parallel electrodes glued between two quartz glass plates. The electrodes were 1 mm thick, 30 mm long, and 1 mm apart from each other. A homemade power supply was connected to one electrode via an RLC (a resistor, an inductor, and a capacitor) circuit and delivered a sinusoidal voltage at 13.56 MHz with a typical root mean square value in the range of a few hundred volts. More

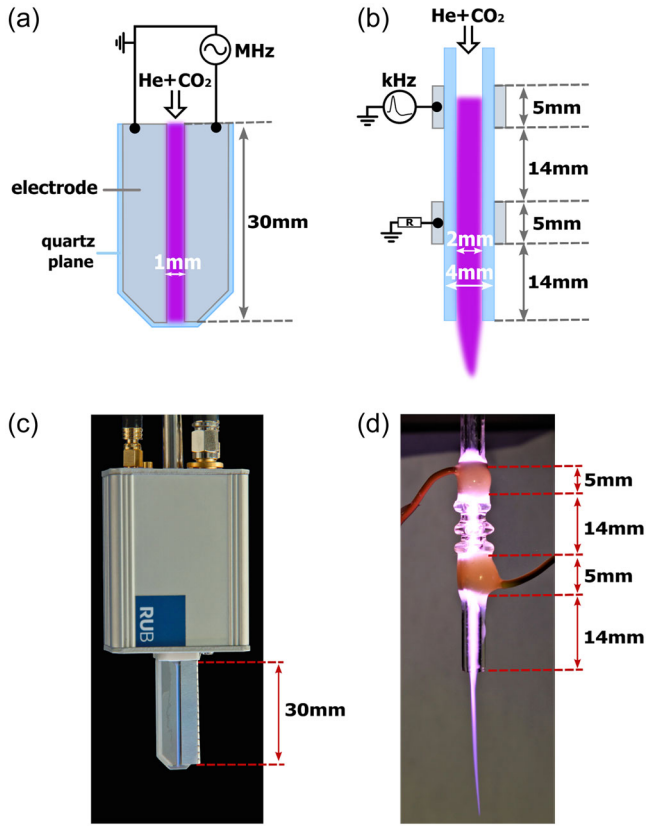

FIGURE 1 Schematic (a) and picture (c) of the MHz-jet used in this study (European Cooperation for Science and Technology (COST) plasma jet). Schematic (b) and picture (d) of the kHz-jet.

TABLE 1 Comparison between the kHz-jet and the MHz-jet parameters.

Parameters	kHz-jet	MHz-jet
Geometry	Coplanar–coaxial DBD	Electrode plan–plan
Propagation in open air (plume)	Plasma	Afterglow
Electrical waveform	Unipolar positive pulse	Sinusoidal
Frequency	20 kHz 3% duty cycle	13.56 MHz
Laplacian electric field direction	∥ to the flow	⊥ to the flow
Electron density	10^{17} – 10^{19} m^{-3}[26–28]	10^{16} m^{-3}[29]

Note: The electron densities are taken from the literature, for the kHz-jet the values are obtained for different setups based on a DBD geometry configuration as the setup presented in this paper and have been estimated in the jet flowing in open air.

Abbreviations: DBD, dielectric barrier discharge.

details about the MHz-jet and the power supply can be found in the paper of Golda et al.[16]

The kHz-jet (Figure 1b) was a coplanar–coaxial DBD reactor. It was composed of a borosilicate glass tube with an outer diameter of 4 mm and an inner diameter of 2 mm. Two copper tapes with a width of 5 mm were wrapped 14 mm apart around the tube. The upper tape was connected to a homemade high-voltage power supply, which delivered a positive microsecond-duration voltage pulse with a kHz repetition rate, where an example of waveform signal is shown in Figure 2. From 2 up to 15 kV, the voltage rise time (defined here between 10% and 90% of the maximum values) and the full width at half-maximum were almost constant, 0.92 ± 0.03 and $1.55 \pm 0.01\,\mu s$, respectively. The lower electrode was wrapped around the tube 14 mm away from the reactor nozzle and connected to a grounded resistor ($R = 100\,\Omega$). The electrodes were separated by three glass beads and isolated by epoxy glue to avoid arc formation in air between the two electrodes, as represented in the picture of Figure 1d.

Both plasma reactors were fed with helium gas (99.999% purity) and mixed with 0% to 1.2% CO_2 (99.9% purity), flowing in a 100–2000 standard cubic centimeter per minute (sccm) range and regulated by calibrated mass flow controllers.

2.2 | Electrical diagnostics: energy consumed by the plasma

The MHz-jet incorporated miniaturized electrical probes inside its housing (see picture in Figure 1c), allowing precise measurement of the voltage applied to the powered electrode and the current leaving the grounded electrode. A 500 MHz bandwidth digital oscilloscope (Tektronix MDO 3054) recorded both signals, and the data were analyzed using a computer to calculate the average power consumed by the plasma, P_{avg}:

$$P_{avg} = V_{RMS} \times I_{RMS} \times \cos(\varphi - \varphi_{ref}), \quad (1)$$

with V_{RMS} and I_{RMS} the effective values of voltage and current, φ the phase shift between voltage and current, and φ_{ref} the instrumental reference phase shift measured experimentally at the same voltage before plasma ignition. The described measuring technique for estimating the power is valid as long as the MHz-jet is operated in stable homogeneous glow mode, which does not exhibit any constricted nanosecond sparks or streamers. More details about the MHz-jet electrical diagnostics can be found in the literature.[16,29]

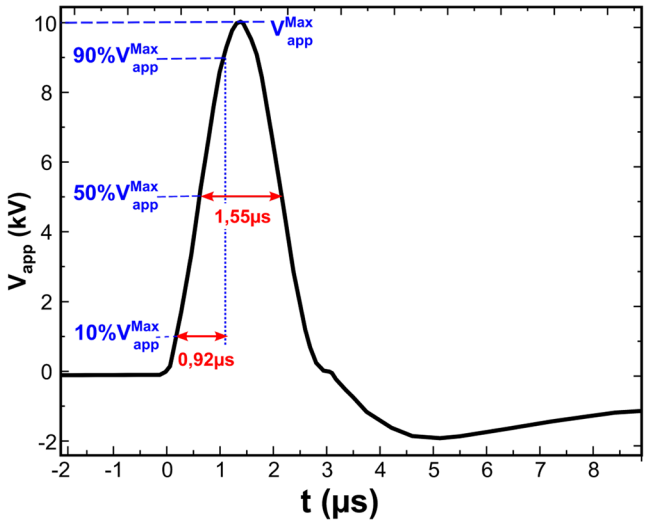

FIGURE 2 Temporal representation of a positive microsecond-duration voltage pulse for the kHz-jet.

For the kHz-jet, the applied voltage (V_{app}) and the cathode current ($I_c = V_c/R$) were measured between the anode (upper electrode) and the ground using a Tektronix P6015A high-voltage probe (75 MHz and 1000:1 division ratio) and across the resistor ($R = 100\,\Omega$) at the cathode (lower electrode) using a LeCroy PP006A voltage probe (500 MHz and 10:1 division ratio). The same oscilloscope as the one used with the MHz-jet recorded both signals. The energy consumed by the plasma during one pulse (E_p) was calculated by integrating the instantaneous power over one period, T:

$$E_p = \int_0^T P(t)dt = \int_0^T V_{app}(t) I_d(t) dt, \quad (2)$$

where I_d is the discharge current. The kHz-jet was a DBD, which means that the current that flows through it consisted of a capacitive current, I_{capa}, and a discharge current, I_d. Without plasma, the reactor acted as a capacitor, meaning that the current that flowed through the reactor was equal to the capacitive current. To measure it, CO_2 gas was flowing through the reactor to make sure that no plasma was ignited. Thus, the discharge current could be estimated from the subtraction of the total current when the plasma was ignited from the capacitive current.[30]

2.3 | Measurement of CO production

The concentration of CO produced by plasma was measured using a gas analyzer (SIEMENS Ultramat23).

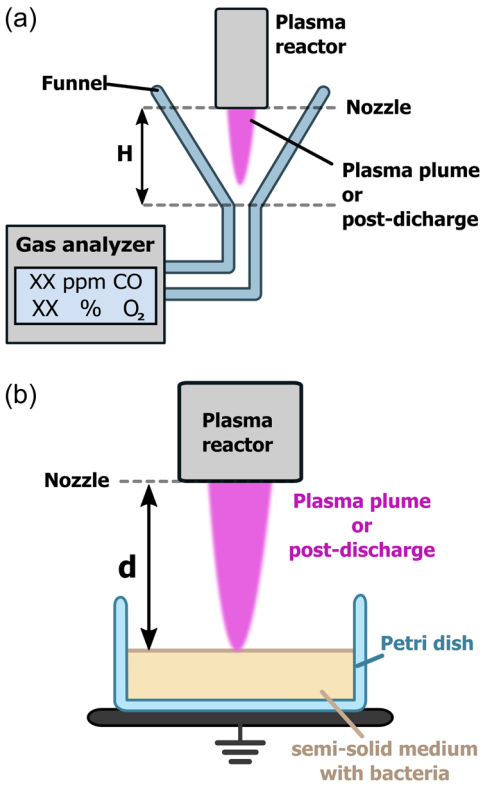

FIGURE 3 Schematics of the measurement setup for CO concentration (a) and the biological treatment (b).

The experimental setup is shown in Figure 3a. A funnel was positioned underneath the reactor and the distance between the funnel's bottleneck and the nozzle of the reactor was 30 mm. The plasma plume for the kHz-jet or the postdischarge for the MHz-jet was positioned inside the funnel, and the analyzer pumped gas samples from the funnel with a gas flow rate between 1000 and 1500 sccm. The sampled volume, $V_{sampled}$, was composed of a gas volume from the exhaust of the plasma, V_{plasma}, and a gas volume from the surrounding air, V_{air}:

$$V_{sampled} = V_{plasma} + V_{air} = x \times V_{sampled} + y \times V_{sampled}, \quad (3)$$

where $x = V_{plasma}/V_{sampled}$ and $y = V_{air}/V_{sampled}$, inducing $x + y = 1$.

The concentration of CO molecules measured by the gas analyzer, $[CO]_{measured}$, is expressed as

$$[CO]_{measured} = \frac{\text{Number of CO molecules produced in the plasma}}{V_{sampled}}, \quad (4)$$

while the concentration of CO molecules in the plasma, $[CO]_{plasma}$, is expressed as

$$[CO]_{plasma} = \frac{\text{Number of CO molecules produced in the plasma}}{V_{plasma}}. \quad (5)$$

By combining Equations (4) and (5), we get

$$[CO]_{plasma} = [CO]_{measured} \times \frac{V_{sampled}}{V_{plasma}} = \frac{[CO]_{measured}}{x}. \quad (6)$$

The parameter x was estimated from y, which was deduced from the measurement of the O_2 molecule concentration, $[O_2]_{measured}$. The dissociation of CO_2 can lead to the formation of O_2 molecules ($CO_2 \rightarrow CO + \frac{1}{2}O_2$). As the maximal value of CO concentration in this work was 1000 parts per million (ppm), the production of O_2 in the plasma could not be higher than 500 ppm, which represents 0.05%. This value, in a first approximation, was negligible compared to the concentration of O_2 in the air, which is 21%. Thereby, we could assume that the concentration of O_2 measured using the gas analyzer, $[O_2]_{measured}$, gave an indication of the ratio of V_{air} over $V_{sampled}$:

$$x = 1 - y = 1 - \frac{[O_2]_{measured}}{[O_2]_{air}} = \frac{[O_2]_{air} - [O_2]_{measured}}{[O_2]_{air}}. \quad (7)$$

Finally, by combining Equations (6) and (7), $[CO]_{plasma}$ is expressed as

$$[CO]_{plasma}\,(\text{ppm}) = [CO]_{measured}\,(\text{ppm}) \times \frac{[O_2]_{air}\,(\%)}{[O_2]_{air}\,(\%) - [O_2]_{measured}\,(\%)}. \quad (8)$$

The measuring range of the gas analyzer was between 0 and 500 ppm with an accuracy of 2 ppm for CO and between 0% and 25% with an accuracy of 0.25% for O_2. The error of $[CO]_{plasma}$ was established from an uncertainty propagation calculation, knowing the accuracy of $[CO]_{measured}$ and $[O_2]_{measured}$.

Since the concentration of CO was not influenced by the time of flight of the gas from the funnel to the gas analyzer, we assumed that $[CO]_{plasma}$ represented the concentration of CO produced in the plasma.

2.4 | Bacteriological treatment

The disinfecting effect of both plasma sources was assessed *in vitro* using a K-12 strain of *E. coli* uniformly seeded on sterile semisolid media of a Petri dish.

To prepare the liquid media, 2 mg/mL lysogeny broth of microbiology powder was dissolved in demineralized water. To prepare the semisolid media, 2.2 mg/mL agarose from microbiology powder must be added to the liquid media solution to ensure solidification. Solutions were sterilized in a conventional autoclave. The semisolid solution was immediately poured by 20 mL per 90 mm diameter Petri dish to obtain 3-mm-thick gels after a 30-min-long solidification. The gels were stored at 4°C overnight before use.

Petri dishes with uniform bacterial layers were prepared in sterile conditions by the inundation method as follows. Stock bacterial solution was taken out from 4°C storage to 16°C ambient air for 10–15 min before use. After homogenization on a vortex stirrer, absorption of the stock solution was measured in sextuplets from 150 µl volumes placed in wells of a 96 multiwell plate. The obtained average absorption value was used to specify the volume that corresponds to 3×10^7 colony forming units with the help of a preliminary established calibration (bacterial counting in sequenced dilutions). This volume was brought to 5 mL by liquid media, poured onto a Petri dish, and left to sit for 20 min. Subsequently, excess liquid was pipetted out and the seeded Petri dish was left open until evaporation of the residual liquid layer.

On each experimental day, Petri dishes were seeded immediately before plasma treatment. One dish per day was kept nontreated as a bacterial control. During treatment, the respective plasma source was placed vertically above the dish at a nozzle-surface distance between 3 and 15 mm as shown in Figure 3b. For each experimental condition, bacterial treatment was performed in triplicates or quadruplicates distributed equidistantly on the same Petri dish. Electrical parameters such as applied voltage and discharge current were recorded simultaneously for each treatment. During treatment, the Petri dish was kept on a grounded alumina plate. Queued dishes were kept at 16°C until their turn. All day's dishes were placed in the incubator at the same time and left overnight for incubation at 37°C. The photos of treated dishes were taken the next day and the surface of each disinfected area was estimated with the help of an image processing software (ImageJ). After that, incubated dishes were discarded as biological waste.

For each plasma condition, all the multiplicates from all day were assembled for statistical analysis represented in the paper in graph form. The data point was calculated as an algebraic mean value and the error bars were calculated using Student's *t*-distribution. Student's *t*-distribution is a useful tool for understanding the statistical behavior of a normally distributed population when the standard deviation is unknown beforehand. It is also known in the literature as *t*-distribution due to a *t* parameter used for the determination of confidence interval α. It allows us to state that with a predefined probability, namely, the confidence interval, the experimental statistical error comprises the true value of the measured value. In summary, Student's distribution is a generalized Gaussian distribution that accounts for a finite number of samples. Brief mathematical derivation and analysis can be found elsewhere.[31] Throughout this work, the confidence interval α was selected to be equal to 0.95, the reference value in biomedical research.[32]

The pH of the plasma-treated seeded semisolid media was measured using litmus paper. The paper was placed on top of the gel immediately after treatment and its color change when soaked served as a pH indicator.

3 | RESULTS AND DISCUSSION

3.1 | Influence of the specific energy on CO production

The SEI is a parameter commonly used to quantify the CO_2 dissociation. It is an intensive parameter that represents the average energy given to each atom or molecule of the gas during one cycle (or pulse). It is defined as

$$SEI\,(\mathrm{J/l}) = \frac{P_{\mathrm{avg}}\,(\mathrm{W})}{\Phi(1/\mathrm{s})} = \frac{E_{\mathrm{p}}\,(\mathrm{J}) \times f\,(\mathrm{Hz})}{\Phi(1/\mathrm{s})}, \qquad (9)$$

where P_{avg} is the average power consumed by the plasma, E_{p} is the energy consumed during one pulse, and Φ is the total gas flow rate at standard conditions ($T_0 = 273.15$ K, $p_0 = 1.013$bar).

The influence of the SEI on the CO_2 dissociation is presented for the two plasma jets in Figure 4 in helium gas with 0.3% admixture of CO_2 with a gas flow rate of 1000 sccm. The left axis represents the concentration of CO in ppm while the right axis depicts the conversion degree defined as $\alpha = \frac{[CO]_{\mathrm{final}}}{[CO_2]_{\mathrm{initial}}}$. SEI was tuned by changing the applied voltage amplitude.

For both jets, the concentration of CO increases with SEI and follows a linear trend up to approximately 50 J/l.

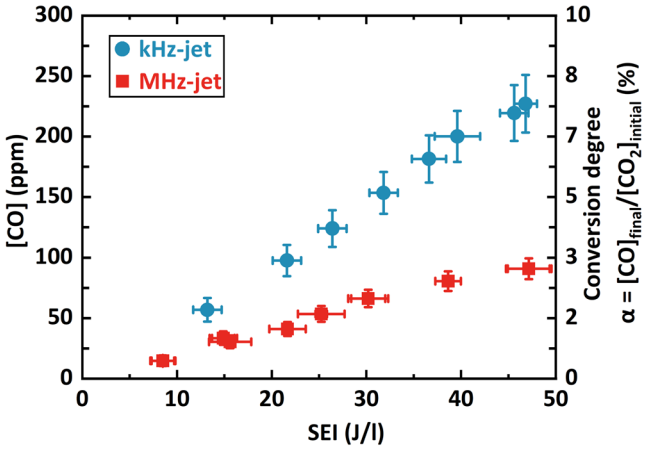

FIGURE 4 CO concentration (left) and CO_2 conversion degree (right) in the MHz-jet (red squares) and in the kHz-jet (blue dot) as a function of the specific energy input (SEI). The data were recorded using a total gas flow rate of 1000 sccm, with 0.3% of CO_2 and a frequency of 20 kHz for the kHz-jet.

At the same value of SEI, the production of CO for the kHz-jet is more than twice the MHz-jet, meaning the conversion is more efficient with the kHz-jet. The CO concentration rose to a maximum of 100 ppm for the MHz-jet and 250 ppm for the kHz-jet. The typical concentration used in CO inhalation clinical trials is from 100 to 4000 ppm. Concentration of 4000 ppm was only tested once, and most of the trials were performed with a concentration from 100 to 500 ppm.[33] One can notice that the CO concentration measured in the two plasma jets was comparable with the one used in CO inhalation clinical trials. This means that the two reactors were safe in terms of CO production.[7]

Three main channels can lead to the dissociation of CO_2 into CO: (1) the dissociation via vibrational up-pumping along the asymmetric mode, (2) direct energetic particle impact involving electrons and excited noble gas species leading to the excitation transfer to CO_2 followed by direct dissociation, and (3) dissociative recombination.[9] While the dissociation via the vibrational up-pumping channel is the most efficient in terms of energy, it does not play a significant role in kHz pulsed DBD as the molecules have time to relax between two pulses.[34,35] However, for the MHz-jet, as there is no extinction of plasma between two cycles, the vibrational up-pumping could play a role. But if this channel was important, as it is the most efficient channel in terms of energy, for the same SEI the production of CO of the MHz-jet would be higher than the kHz-jet's. As it is not the case, we can conclude that the vibrational up-pumping dissociation was not the main process to produce CO in the MHz-jet. This observation is not surprising since here the gas is mainly composed of

helium with only a small admixture of 0.3% CO_2. Vibrational up-pumping requires frequent collisions between CO_2 molecules. However, due to the dilution in helium, a lot of de-exciting collisions with helium atoms occur, so the vibrational up-pumping was hindered.

The backward reaction of CO with O_2 to form CO_2 is negligible when the temperature does not exceed 3000 K.[9] CO is also not easily oxidized or reduced,[35] which makes this molecule very stable in time in the gas phase. To make sure that CO molecules were not lost in the gas phase, the concentration was measured versus the time of flight of the gas from the plasma to the gas analyzer. We checked that the number of CO molecules was not influenced, meaning that the processes involving long-lifetime molecules were negligible here.

The discrepancy in terms of CO production for the two plasma sources can be explained by multiple factors. The first assumption is related to the dissociation process itself; indeed, the values issued from the literature and shown in Table 1 indicate a difference in the electron density of at least one order of magnitude between the kHz-jet and the MHz-jet. When considering the direct electron impact as a potential mechanism participating in the dissociation, this difference in density would play a major role with those higher densities enhancing the production of CO with the kHz-jet. Their role could also be indirect, with first the excitation of the noble gas and then colliding with CO_2.

A second possibility is related to the loss process. In the plasma phase, the loss of CO due to electron impact dissociation is negligible because it requires about twice as much energy as the electron impact dissociation of CO_2,[35] and the electron impact ionization of CO is not important if the percentage of CO is less than 15% (*i.e.*, 150 000 ppm), which is the case of the present study. CO can be lost by two backward reactions involving the atomic oxygen O via three-body reaction or the negative ion O^- via electron detachment.[34] In helium plasma jets, O^- is one of the dominant negative ions.[36] Generally, negative ions have a longer lifetime than positive ions since positive ions can recombine with electrons.[37] But O^- and O are very reactive and form other species quickly. Since their lifetimes are very short, when the residence time in plasma is lower than hundreds of ms, the backward reactions involving these two species are negligible.[34] In the case of the kHz-jet, as the duration of the plasma did not exceed 1 μs, we can assume there was no CO backward reaction. With the MHz-jet, such a statement cannot be made since the plasma never extinguishes between two successive cycles, meaning the residence time depends on the gas flow. The latter was 1000 sccm and the plasma area was 30 mm long with a diameter of 1 mm (cf. Figure 1a). By assuming a circle cross-section of the reactor, the gas would need more than 1 ms to leave the plasma area. As this time is longer than in the kHz-jet, it could explain why the concentration of CO is less with the MHz-jet than with the kHz-jet: backward reactions with O^- and O may occur with the MHz-jet and therefore decrease the number of CO molecules.

The mechanisms involved in those two setups depend on many factors. To unravel the complexity of the chemistry involved and the difference in efficiency, more experimental data would be needed regarding the composition of the species in the discharges.

3.2 | Influence of the percentage of CO_2 on the CO production

To evaluate the role of the CO_2 concentration in the feed gas, CO concentration and the conversion degree were measured as a function of the CO_2 admixture at a constant SEI chosen at 52 J/l. Both reactors were fed with helium at 500 sccm. Figures 5 and 6 present the concentration of CO and the conversion degree as a function of the CO_2 admixture, respectively.

For the MHz-jet the concentration of CO increased gradually with increasing concentration of CO_2 up to 0.6% and reached a plateau at around 200 ppm. The trend of the kHz-jet was different. Even at the lowest studied

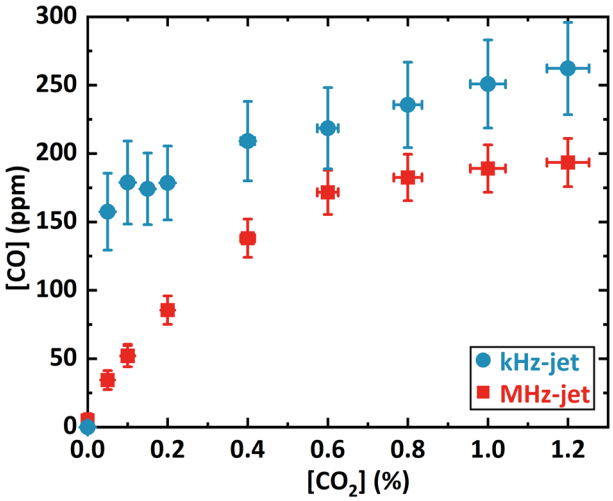

FIGURE 5 CO concentration as a function of the CO_2 percentage for the MHz-jet (red squares) and the kHz-jet (blue dots). The data were recorded for a specific energy input (SEI) of 52 J/l, using a total gas flow rate of 500 sccm and a frequency of 20 kHz for the kHz-jet.

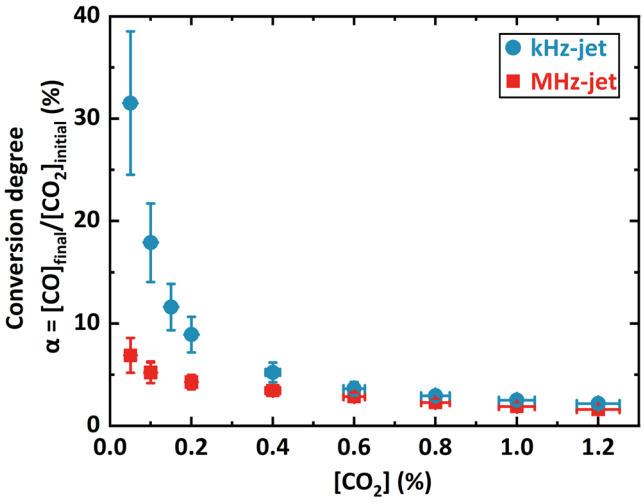

FIGURE 6 Conversion degree of CO_2 as a function of the CO_2 percentage for the MHz-jet (red squares) and the kHz-jet (blue dots). The data were recorded for a specific energy input (SEI) of 52 J/l, using a total gas flow rate of 500 sccm and a frequency of 20 kHz for the kHz-jet.

CO_2 percentage, CO concentration was already at 150 ppm. Note that at 0%, the gas analyzer did not measure any CO molecules. The concentration followed a linear increase as a function of the CO_2 percentage. By taking into account the error bars, when the CO_2 percentage was above 0.6%, the concentrations of CO were comparable for the two plasma jets.

From Figure 6, it can be noticed that the conversion degree decreased with the CO_2 concentration. The main reason for this observation is probably due to the energy loss of electrons in the rotational and vibrational states of CO_2.

To fully understand the differences in CO production and destruction for the two plasma discharges, a full-plasma chemical model taking into account the excitation mechanisms and the resulting plasma chemistry would be necessary. This would also give an idea about the other relevant plasma species for disinfection, as specified in the following sections.

3.3 | Feed gas bacterial controls

To ensure that the bactericidal effect following plasma treatment was not caused by gas flow itself by lack of oxygenation or local pressure increase, feed gas controls have been performed. For that purpose, the kHz-jet was placed at a nozzle-surface distance of 5 mm and flushed with neutral gas.

Figure 7 shows same-scale photographs after overnight incubation of the following feed gas control treatments: helium, argon, helium with 21 000 ppm CO_2 admixture and a gas flow of 500 sccm for 10 min, and argon with 1000 ppm CO admixture and a gas flow of 1000 sccm for 15 min (from left to right). The CO admixture in CO-containing gas control was selected to be superior to what any studied plasma treatment can create (as shown in Figure 5). Each photo represents a square with a side of 4.5 cm showing one quarter of a Petri dish.

No effect on bacterial proliferation was observed for any gas control. For CO, this result shows that in our conditions there was no contribution of gaseous CO to bacterial inactivation. At the same time, according to the literature, an antibacterial feature of CO was mainly observed with CO-releasing molecules and not with CO gas.[23,25]

3.4 | pH of the plasma-treated surface

Each bacterium has its own range of acidity compatible with life and reproduction, and any exposure that goes beyond this range can lead to various inhibition effects, including slowed growth, cell cycle arrest, or cellular death.[38] For *E. coli*, this range lies between 4.5 and 9.[38] Plasma is known to modify the properties of treated media, including, among others, the acidity of water-containing media.[39] In this regard, since the Petri dish is largely constituted with water, the change in acidity was measured on the gel's surface immediately after plasma treatment. It was observed in our conditions that acidity decreased from 7 to 6 in a zone with a diameter of about 3 mm below the nozzle. Thus, plasma disinfection could not be caused by acidity change since the change was within the *E. coli*'s accepted range of pH. Apart from that, at further reading of the article, it will also be noted that the acidity change zone was way smaller than almost any disinfected area.

3.5 | Influence of helium plasma treatment time on bacterial disinfection

First, the disinfection efficiency of plasma sources as a function of time was evaluated in pure helium without admixture of CO_2. The flow and SEI were fixed at 500 sccm and about 50 J/l, respectively. The nozzle-surface distance was kept at 5 mm and the bacterial sample's treatment time varied from 30 s up to 8 min. Such distance and time values were chosen based on their frequent appearance in the literature.[40]

Figure 8 shows same-scale photographs of typical disinfected areas after overnight incubation following the

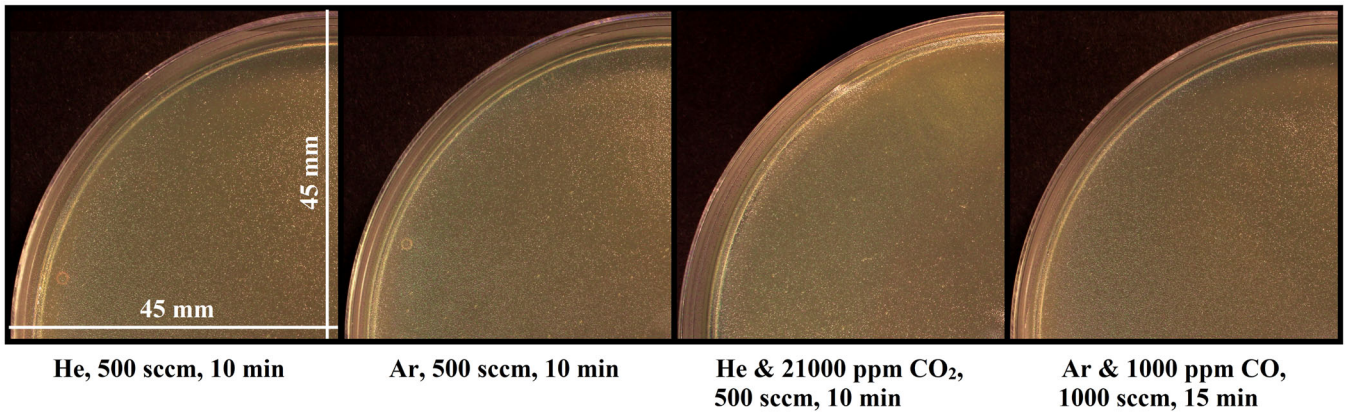

FIGURE 7 Same-scale photographs of *Escherichia coli* treated by helium, argon, and helium with 21 000 ppm CO_2 admixture at a gas flow of 500 sccm for 10 min, and argon with 1000 ppm CO admixture at a gas flow of 1000 sccm for 15 min.

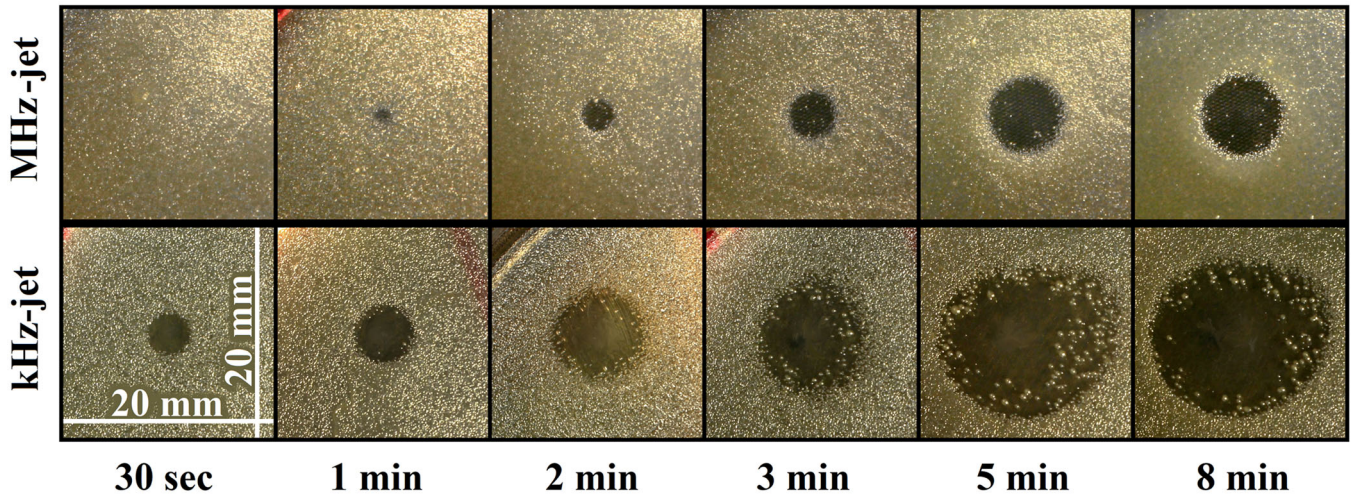

FIGURE 8 Same-scale photographs of disinfected areas of plasma-treated *Escherichia coli* by the MHz-jet (top line) and kHz-jet (bottom line) as a function of time. The data were taken at 500 sccm helium gas flow rate at 5 mm nozzle-surface distance. For the kHz-jet, the frequency was set to 20 kHz.

above-specified helium plasma treatment by MHz-jet (top line) and kHz-jet (bottom line) for 30 s, 1 min, 2 min, 3 min, 5 min, and 8 min (columns from left to right). Each photo represents a square with a side of 2 cm. Figure 9 reunites the data on disinfected areas as a function of time performed in multiplicates (from three to four samples per condition).

It is apparent from Figures 8 and 9 that both plasma sources govern a monotonous increase of disinfected area with time, with a larger area for the kHz-jet treatment compared to MHz-jet for all tested times. In addition to that, both sources appear to reach their maximum disinfection efficiency at about 5 min since at longer times there was almost no area increase. For this reason, all subsequent bacteriological experiments were carried out with a duration of 5 min.

Despite similar temporal disinfection trends between kHz-jet and MHz-jet, there was a difference in a superficial distribution of survived colonies, as can be observed in Figure 8. For MHz-jet, isolated survived colonies can be found at any point in the disinfected area, and the area's borderline width stays rather constant. For kHz-jet, however, survived colonies can be only found near the border, and the longer the treatment time, the wider the border becomes.

3.6 | Influence of nozzle-surface distance on bacterial disinfection

Second, the disinfection efficiency of plasma sources as a function of nozzle-surface distance was evaluated in

helium with 0.6% admixture of CO_2 as feed gas. Two distinct cases of flow and SEI were studied: 500 sccm at about 50 J/l and 250 sccm at about 100 J/l. The treatment time was kept at 5 min. The nozzle-surface distance varied from 3 mm up to 15 mm.

Figure 10 shows same-scale photographs of disinfected areas after overnight incubation following the above-specified He-CO_2 plasma treatment by MHz-jet (top line) and kHz-jet (bottom line) at nozzle-surface distances of 3, 5, 7, 10, and 15 mm (columns from left to right). Each photo represents a square with a side of 2 cm. Figure 11 reunites the data on disinfected areas as a function of nozzle-surface distance performed in multiplies (from three to 11 samples per condition).

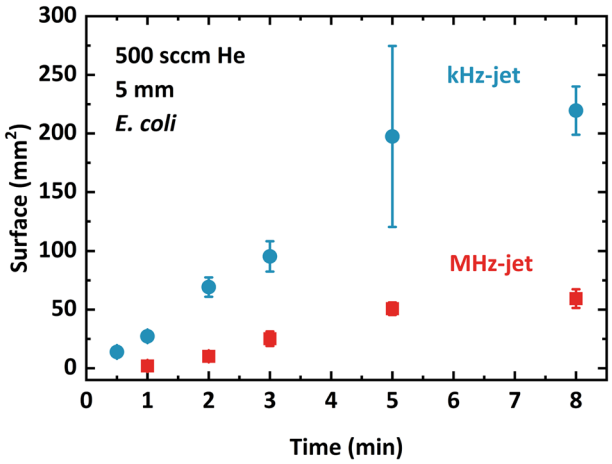

FIGURE 9 Surfaces of disinfected areas during plasma treatment by the MHz-jet (red squares) and the kHz-jet (blue dots) as a function of time. The average specific energy input (SEI) value was kept at 50 J/l. The data were taken at 500 sccm helium gas flow rate at 5 mm nozzle-surface distance. For the kHz-jet, the frequency was set to 20 kHz.

The border of disinfected areas and survived colonies' distribution stay in agreement with the time scan in helium shown in Figure 8. Overall, at any tested distance, disinfection in He-CO_2 feed gas was more effective by the MHz-jet than by the kHz-jet. It is the opposite trend from the one observed in plasma fed by He gas only (cf. Figures 8 and 9).

For the kHz-jet, the disinfection area increased with nozzle-surface distance from 3 to 5 mm, stayed rather constant in the region between 5 and 10 mm, and slightly decreased from 10 to 15 mm. The presence of maximum might be linked to the species created in the ambient air—at shorter distances they are not created enough along the plasma plume, while at longer distances they do not arrive at the substrate and are quenched by air molecules. The declining character of the slope at larger distances is intuitively expected—when the source is too far away from the target, no action can be brought to the latter.

For the MHz-jet, however, the disinfected area monotonously increased with distance. At 3 mm, the area presented not axial but planar symmetry, which is no longer observed at distances greater than 5 mm.

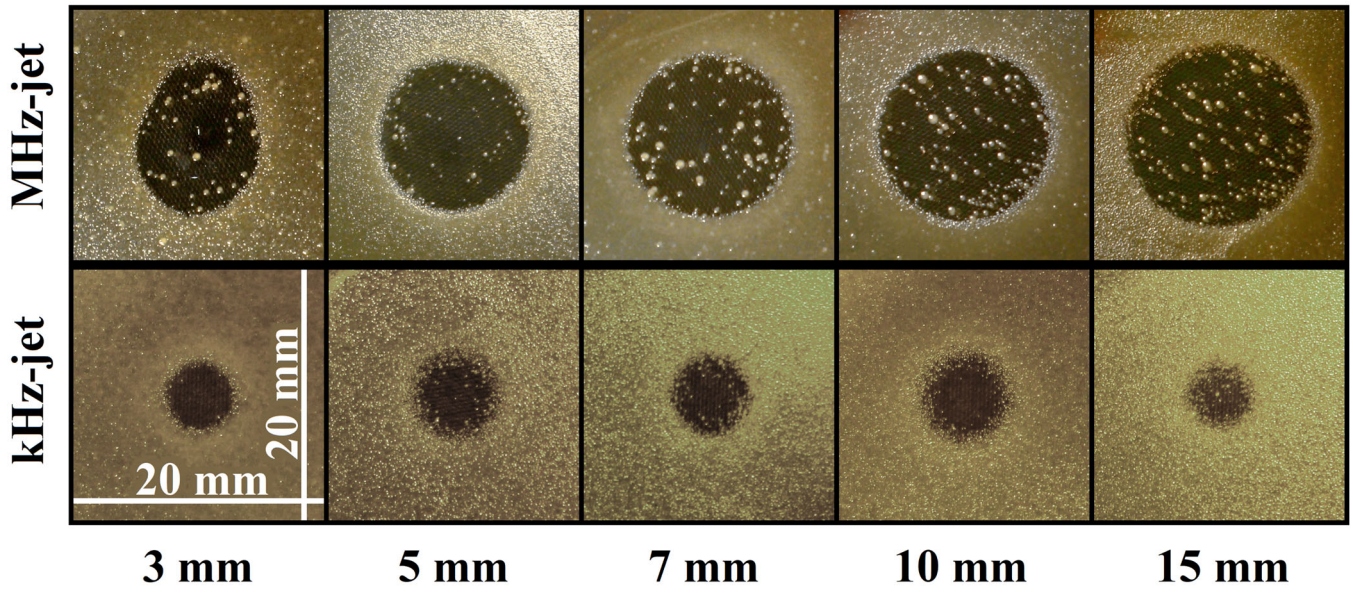

FIGURE 10 Same-scale photographs of disinfected areas of plasma-treated *Escherichia coli* by the MHz-jet (top line) and kHz-jet (bottom line) as a function of nozzle-surface distance. The data were taken at 500 sccm helium/0.6% CO_2 gas flow rate for 5 min plasma treatment. For the kHz-jet, the frequency was set to 20 kHz.

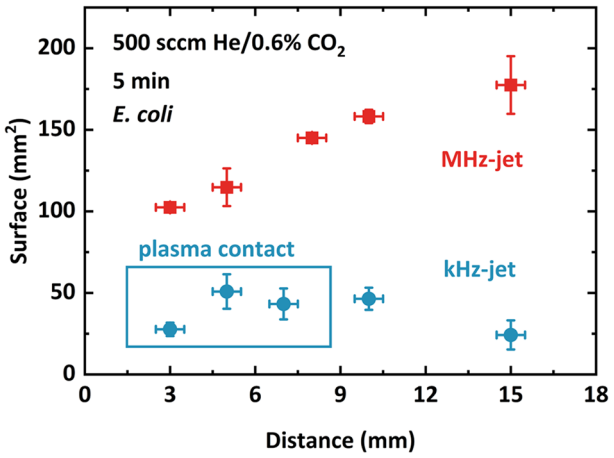

FIGURE 11 Surfaces of disinfected areas during plasma treatment by the MHz-jet (red squares) and the kHz-jet (blue dots) as a function of nozzle-surface distance. The average specific energy input (SEI) value was kept at 50 J/l. The data were taken at 500 sccm helium/0.6% CO_2 gas flow rate for 5 min plasma treatment. For the kHz-jet, the frequency was set to 20 kHz.

It might be due to a slight tilt of the plasma jet that causes an asymmetric flow pattern due to the buoyancy of helium in air or due to the rectangular shape of MHz-jet's gas outlet, which could have an impact on the afterglow's spatial distribution in the nozzle's vicinity.

When interpreting these results, one should also take note of the following differences between plasma sources. MHz-jet was a plane–plane discharge generated in gas flow between two metal plates confined by a pair of quartz slides. In such a case, plasma remains inside the reactor, and its gas outlet is composed of plasma afterglow only. Meanwhile, the kHz-jet was a coplanar–coaxial DBD. Once ignited inside the capillary, plasma follows the gas flow and forms a centimeter-scale long plume outside the nozzle. Thus, at some nozzle-surface distances, the plasma plume might touch the agar substrate of a Petri dish. The length of the plume depends on multiple plasma parameters, including feed gas composition and SEI. For 0.6% CO_2 admixture, for 500 sccm flow at 50 J/l, electrical contact was present at nozzle-surface distances shorter than 8 mm, as shown in Figure 11, while for 250 sccm flow at 100 J/l, contact was present at nozzle-surface distances shorter than 3 mm. The point of contact is submillimetric in diameter.

Figures 10 and 11 show the data for plasma treatments with feed gas flow of 500 sccm and SEI at about 50 J/l only, but all the discussed above was as well observed for plasma treatments with feed gas flow of 250 sccm and SEI at about 100 J/l (data not shown).

3.7 | Influence of CO_2 ratio on bacterial disinfection

Finally, the disinfection efficiency of plasma sources as a function of the CO_2 admixture was evaluated at two distinct cases of flow and SEI: 500 sccm at about 50 J/l and 250 sccm at about 100 J/l. For each SEI value, two nozzle-surface distances were studied: 5 and 10 mm. The treatment time was kept at 5 min.

Figure 12 reunites the data on disinfected areas measured following the above-specified He-CO_2 plasma treatment by kHz-jet and MHz-jet as a function of CO_2 admixture from 0.0% to 1.2% performed in multiplicates (from three to 16 samples per condition).

Figure 12 displays the effect of CO_2 admixture to feed gas on bacterial disinfection by kHz-jet and MHz-jet plasma sources. Below a CO_2 admixture of 0.2%, the disinfection efficiency decreased for kHz-jet and, inversely, increased for MHz-jet. Thus, the admixture of CO_2 to the feed gas has the opposite effect in the two plasma sources.

Figure 12 shows the data for plasma treatments with feed gas flow of 500 sccm and SEI at about 50 J/l at 5 mm distance only, but all the discussed above was as well observed for other plasma treatments, namely: (i) with 500 sccm and 50 J/l at 10 mm, (ii) with 250 sccm and 100 J/l at 5 mm, and (iii) with 200 sccm and 100 J/l at 10 mm (data not shown).

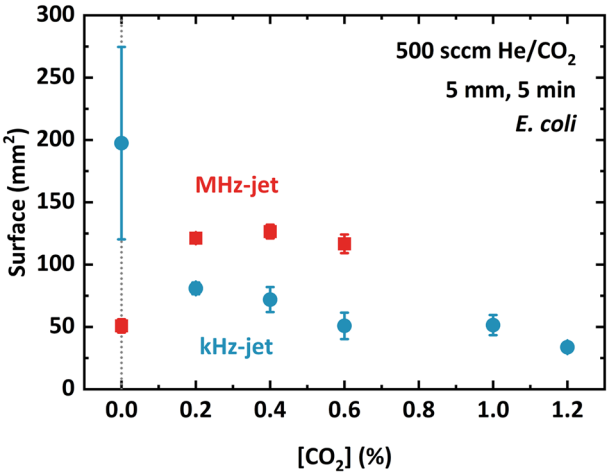

FIGURE 12 Surfaces of disinfected areas during plasma treatment by the MHz-jet (red squares) and the kHz-jet (blue dots) as a function of CO_2 concentration. The vertical dotted line corresponds to pure He plasma treatment. The average specific energy input (SEI) value was kept at 50 J/l. The data were recorded at 500 sccm helium/CO_2 gas flow rate at 5 mm nozzle-surface distance for 5 min plasma treatment. For the kHz-jet, the frequency was set to 20 kHz.

3.8 | Discussion on antibacterial properties of plasma

These results show that even if the gas mixture, the flow, and the SEI were identical, the comparison of these two plasma sources remains a challenge. Even if the control parameters are similar, the physics of these two plasma jets are very different due to the different excitation waveform and electrode geometry and thus producing different effects on bacteria. But despite this, both plasma jets exerted antibacterial properties even with the addition of CO_2 in the gas mixture. It is a promising result since it demonstrates that the plasma can produce CO for anti-inflammatory purposes and at the same time be bactericidal.

Plasma is a cocktail of many components such as charged species, UV radiation, electric field, and radical and chemical products including reactive species.[41,42] It represents a great advantage since it brings together many components that would be complicated to produce in other conditions, and their interaction with biological targets opens the opportunity for synergistic effects. However, at the same time, this cocktail is also a drawback for the interpretation of the results since it is a real challenge to isolate the effects of each component.

For the kHz-jet, as in some cases the plasma had direct contact with the target, all plasma components such as reactive neutrals, charged species, electric field, or UV radiation could interact with *E. coli*, while for the MHz-jet the plasma plume was a postdischarge, meaning that only UV radiation and radical and chemical products could interact with the bacteria.

The rich chemistry of plasma can induce a pH change and affect the viability of bacteria. In our case, pH measurement on the gel indicated that it decreased at a minimal value of 6. This value was in the range of acidity tolerance of *E. coli*, which is from 4.5 to 9,[38] meaning that the acidity was not the reason for the bactericidal properties of the plasma.

The temperature is an important parameter in any biological applications and it is required to not cross 42. 5°C to avoid the denaturation of proteins.[43] *E. coli* strain can survive at higher temperatures and its inactivation temperature is at around 60°C.[44]

In pure helium, the gas temperature in the plasma of the MHz-jet, when operated at typical parameters, increases above 45°C.[45] However, when the effluent hits the target the gas has cooled down significantly, so we can assume that the temperature at the target did not exceed 42. 5°C. For the kHz-jet, as each group has its own plasma jet, the estimation of the gas temperature is complicated. It has been shown that the temperature surface increases with the leakage current by Joule heating.[46,47] It means that the target temperature depends on the type of power supply. As the influence of the CO_2 addition on the temperature has never been estimated in these conditions (as far as we know), we measured it.

A fiber optic temperature sensor (Optocon Fotemp) was inserted in the agarose gel at less than 1 mm deep in the center of the plume spot (location where the plume hit the surface). The temperature was measured for the kHz-jet (blue) and the MHz-jet (red) with three different CO_2 admixtures: 0% (full symbol), 0.6% (open symbol), and 1.2% (cross symbol), and the results are presented in Figure 13.

In any case, the gas temperature increased with the treatment time. Similar behavior has been observed by Lotfy.[48] It was due to the required time to reach thermal equilibrium between the target and the gas. The influence of the CO_2 ratio on the temperature is not obvious, since there is no monotonic relationship between the CO_2 ratio and the temperature. For the MHz-jet, the temperature was higher with no CO_2 admixture, but the temperature with 1.2% CO_2 was higher than with 0.6% CO_2. For the kHz-jet, the behavior was even different, since the temperature was quite similar for 0% and 0.6% of CO_2, while it was lower at 1.2% CO_2. For the latter case, the decrease in the temperature could be explained by the decrease in the length of the plasma plume with the addition of CO_2 gas. At 1.2% CO_2, the plume was barely in contact with the target. However, to understand the exact role of the addition

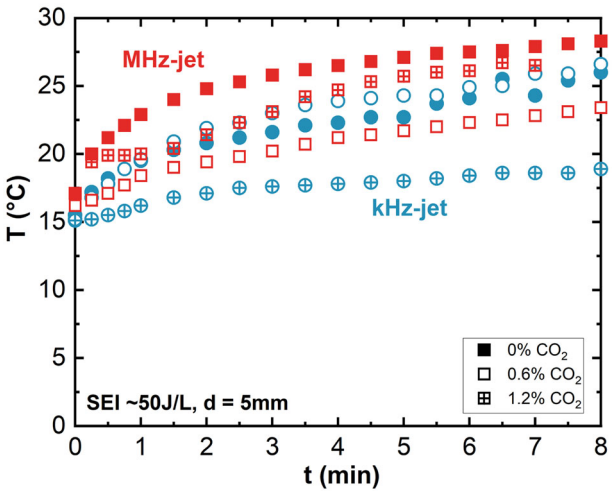

FIGURE 13 Temperature of the agarose gel at the center of the plume spot as a function of the treatment time for the kHz-jet and the MHz-jet at various CO_2 admixtures. The average specific energy input (SEI) value was kept at 50 J/l. The data were recorded at 500 sccm helium/CO_2 gas flow rate at 5 mm nozzle-surface distance. For the kHz-jet, the frequency was set to 20 kHz.

of CO_2 gas on the temperature, a dedicated study on it is needed, which is out of the scope of this paper.

In any case, these results demonstrate that the temperature of the target was lower than 30°C. Therefore, the temperature was not a potential cause of bacteria inactivation in this study. Additionally, these results show that both jets remain safe in terms of temperature for biological targets even with the addition of CO_2.

As there is a rich database of measured absolute densities of reactive species for the MHz-jet and their temporal and spatial dependencies are easy to interpret due to the afterglow character of the effluent, we will discuss their potential influence and antibacterial effects first.

Figure 11 shows that the disinfected area increased with the nozzle-surface distance for the MHz-jet, which indicates that long-lifetime reactive species must be responsible for the bacterial properties. Furthermore, this area increased with the CO_2 admixture (cf. Figure 12), which means that the addition of the CO_2 molecules must increase the amount of the long-lifetime reactive species responsible for the bactericidal properties. This excludes, for example, charged species that are negligible in the effluent of the MHz-jet.[12] We observed experimentally that the amount of CO_2 molecules dissociated by plasma increased with the percentage of CO_2 in the gas mixture (Figure 5), and this dissociation leads to the production of a CO molecule and an O atom.

CO is very stable in time, meaning that this molecule can travel long distances, and in some conditions, these molecules can inactivate bacteria.[23,25] We showed that treatment with gaseous argon with 1000 ppm of CO for 15 min had no effect on *E. coli*. As both plasma jets produced less than 1000 ppm of CO, we can conclude that this neutral molecule was not responsible for the bactericidal properties of plasma. However, for the kHz-jet, we cannot completely neglect that excited CO or CO ions could have an effect.

Atomic oxygen is known to be very reactive and able to inactivate bacteria.[49] But its high reactivity makes its lifetime very short; as a result, its density decays exponentially in the effluent.[50,51] It means that this atom may not be the main species responsible for the bactericidal properties of the MHz-jet. However, the dominant recombination process of O is the three-body reaction with O_2 to form ozone (O_3).[52] O_3 has strong antibacterial properties and a long lifetime.[53] Its half-life is in the range of hours up to days, depending on the temperature, humidity, and airspeed.[54] Ellerweg et al. measured in a similar MHz-jet fed with helium and oxygen admixture that the concentration of ozone increased with the distance from the nozzle in the effluent.[55] In the effluent, as there is no plasma, the atomic oxygen rapidly recombines with oxygen molecules to produce ozone, which explains why the amount of O atoms falls rapidly while the amount of O_3 increases in the effluent.[56] These results agree well with studies in the literature that similarly suggest ozone as an effective disinfection agent for *E. coli* bacteria.[57–59] For example, Pavlovich et al. demonstrated that antibacterial effects on *E. coli* from indirect air DBD treatment of water directly correlate with the measured ozone density in the gas phase.[57] Additionally, the amount of ozone produced in the plasma with increasing CO_2 admixture directly correlates to the disinfection surface trend observed in our experiments.[12] Therefore, ozone is an excellent candidate to explain the antibacterial properties of the MHz-jet.

O atoms can also be converted into O_2, and via the electron impact excitation of this molecule it can form singlet delta oxygen ($O_2(^1\Delta)$), which is the main production path of this reactive species.[60] Singlet delta oxygen is considered a long-lifetime reactive species and can reach up to 75 min in the gas phase.[61] Additionally, it exhibits antibacterial properties[61,62] and can also make a good candidate to explain the bacteria inactivation of the MHz-jet.

Hydroxyl radicals (OH) are also molecules considered responsible for antibacterial effects and they may also be produced in the plasma. However, the main production channel of OH is from electron impact dissociation of water. As there is no water admixed to the feed gas, the amount of OH produced in the plasma is negligible.[63] Additionally, Benedikt et al. determined the OH density in the effluent of the MHz-jet using cavity ring-down spectroscopy and mass spectrometry: both diagnostics show a decreasing trend with increasing distance from the nozzle. This indicates that in the case of the MHz-jet, OH is not the dominant species for the observed antibacterial effects.[63]

Impurities in the gas could produce other species able to inactivate bacteria, but this is unlikely since the plasma area is confined between the two electrodes where there is no direct contact with air. Ellerweg et al. did not measure any atomic oxygen or ozone in the effluent of a MHz-jet when no O_2 was added to the gas mixture.[55] A similar observation was made with NO and N_2O by Douat et al. and they showed that the production of these species requires the addition of nitrogen.[64] This reinforces the fact that impurities in trace amounts do not produce significant amounts of reactive species to inactivate bacteria.

UV radiation can be involved in bacteria inactivation. Golda et al. demonstrated that vacuum ultraviolet (VUV) produced by helium excimers are present in helium MHz-jet.[65] VUV light is absorbed by air, but thanks to

the plume a helium channel links the jet with the target and allows the photons to reach the bacteria. Plasma-generated VUV photons can play a role in the inactivation of bacteria as shown by Schneider et al.[66] But the inhibition zone only had the size of the irradiation zone, which was approximately $2 \times 2\,mm^2$. Additionally, they showed that the admixture of molecular gases (in their case, nitrogen or oxygen) notably reduces since the VUV excimer continuum was strongly quenched due to pooling reactions of metastables with molecular species.[65] The addition of CO_2 gas must have a similar effect. Therefore, we can conclude that in our conditions, UV photons might play a minor role in *E. coli* inhibition.

As all the plasma components can be responsible for the bactericidal effect of the kHz-jet, the interpretation of the results is harder. Figure 11 shows that when the kHz-jet did not have direct contact with the bacteria (from 8 to 15 mm), a bactericidal effect is still observed, which means that long-lifetime reactive species and/or UV play a role in the bacteria inactivation. As shown in Figure 12, the disinfected area decreased with the addition of CO_2 in the gas mixture, while it is the opposite with the MHz-jet. The plume of the kHz-jet is a plasma, which means that in pure helium, reactive oxygen and nitrogen species (RONS) were produced at the interface of the plume with the surrounding air, while it was not the case with the MHz-jet and may explain why the bacteria inactivation was more pronounced in pure helium with the kHz-jet than with the MHz-jet. The addition of CO_2 may add a weak contribution to the RONS production for the kHz-jet, while it is an important one for the MHz-jet.

For the kHz-jet, the results are not as easy to interpret as the plasma chemistry in the effluent is more complex than in the MHz-jet due to the active plasma character. The amount of CO molecules produced by plasma does not follow the trend of the disinfected area as a function of the CO_2 percentage for the kHz-jet (Figures 5 and 12), while it is the case of the MHz-jet. It suggests that the plasma components responsible for the antibacterial properties of the kHz-jet are hindered by the addition of CO_2 in the gas mixture. This might hint, for example, at charged species being responsible whose density probably decreases with higher CO_2 admixtures. Different disinfection mechanisms for both discharge types might also explain the different observed patterns regarding surviving bacteria colonies in the disinfection area as, for example, observed in Figure 10.

In summary, long-lifetime reactive species are probably the main ones responsible for the antibacterial properties of the MHz-jet, and the two probable species involved are ozone and singlet delta oxygen. For the kHz-jet, long-lifetime reactive species must also play a significant role, but the other plasma components such as the electric field and the charged and short-lifetime species cannot be neglected. For both jets, UV photons must play a role in bacteria inactivation but only in pure helium, since UV emission must be reduced by the addition of molecular gases. The amount of dissociated CO_2 molecules improved the antibacterial properties of the MHz-jet, while it is the opposite for the kHz-jet.

4 | CONCLUSION

As CO is a stable molecule and has anti-inflammatory properties, its production by plasma could be a significant advantage in the field of plasma medicine. For this purpose, this paper presents a comparative study of the CO production of two different plasma jets: a MHz generated by the COST reactor and a kHz generated by a coplanar–coaxial DBD reactor. Both plasma sources were fed with helium gas with various amounts of CO_2 admixture from 0% to 1%. CO molecules were produced by the dissociation of CO_2 by plasma, and their concentration was measured by a gas analyzer using an IR absorption spectroscopy method.

The production of CO could be tuned from a couple of ppm to several hundreds of ppm and ensures that the two plasma sources were safe for clinical applications. The concentration of CO produced by plasma as a function of the SEI at fixed CO_2 concentration followed a linear trend. For the same SEI, the production of CO was more efficient for the kHz-jet than the MHz-jet. It could be due to the higher electron density in the kHz-jet as well as the backward reaction involving atomic oxygen and negative oxygen ions, since this reaction is negligible in kHz excitation while it is not the case with MHz excitation.

The conversion degree decreases with the CO_2 concentration in the gas mixture and was probably due to the energy loss of electrons in the rotational and vibrational states of the CO_2 molecules.

Both plasma jets exhibit antibacterial properties on *E. coli* K-12 strain in pure helium and with the addition of CO_2 in the gas mixture. This is a promising result since it demonstrates for the first time that the plasma can produce CO for anti-inflammatory purposes and at the same time be bactericidal. We showed that long-lifetime reactive species were probably the main responsible plasma component for the antibacterial properties of the MHz-jet. The two probable species involved were ozone and singlet delta oxygen. For the kHz-jet, long-lifetime reactive species also play a significant role, but the other plasma components such as the electric field, the charged particles, and short-lifetime species cannot be neglected. For both jets, UV photons must play a role in bacteria inactivation but only in pure helium, since

UV emission must be reduced by the addition of molecular gases. The amount of dissociated CO_2 molecules improved the antibacterial properties of the MHz-jet, while it is the opposite for the kHz-jet. This highlights the challenges in comparing different plasma sources and their effect: even if the control parameters such as feed gas admixture and SEI are the same, biological results may completely differ. This underlines the necessity of careful plasma characterization.

AUTHOR CONTRIBUTIONS

Claire Douat and Judith Golda: Conceptualization. **Eloïse Mestre, Inna Orel, Daniel Henze, Laura Chauvet, Sebastian Burhenn, Judith Golda, and Claire Douat**: Writing—original draft presentation. **Sébastien Dozias:** Design of the power supply. **Eloïse Mestre, Inna Orel, Daniel Henze, Laura Chauvet, Sebastian Burhenn, Fabienne Brulé-Morabito, Judith Golda, and Claire Douat**: Methodology and data interpretation. **Eloïse Mestre, Daniel Henze, Laura Chauvet, and Sebastian Burhenn**: Chemical and electrical data acquisition. **Eloïse Mestre and Daniel Henze**: Chemical and electrical data treatment. **Inna Orel**: Biological data acquisition and treatment. **Eloïse Mestre, Inna Orel, Daniel Henze, Laura Chauvet, Sebastian Burhenn, Fabienne Brulé-Morabito, Judith Golda, and Claire Douat**: Writing—review and editing. All authors discussed the results, reviewed the manuscript, and have read and agreed to the published version of the manuscript.

ACKNOWLEDGMENTS

The authors would like to thank the French Research Agency, ANR (MediCO-Plasma|ANR-21-CE19-0005) for funding this research and the French program PHC Procope (48122NF) and the German program DAAD for funding the travel expenses of this collaboration. This work was also funded by the German Research Foundation in the PlasNOW project as well as CRC 1316, projects B2 and B11.

DATA AVAILABILITY STATEMENT

The data that support the findings of this study are available from the corresponding author upon reasonable request.

ORCID

Inna Orel https://orcid.org/0000-0002-7071-889X
Laura Chauvet https://orcid.org/0000-0003-2510-0377
Sebastian Burhenn https://orcid.org/0000-0002-1254-0886
Judith Golda http://orcid.org/0000-0003-2344-2146
Claire Douat http://orcid.org/0000-0001-9964-4313

REFERENCES

[1] P. J. Bruggeman, F. Iza, R. Brandenburg, *Plasma Sources Sci. Technol.* **2017**, *26*(12), 123002. https://doi.org/10.1088/1361-6595/aa97af
[2] M. G. Kong, G. Kroesen, G. Morfill, T. Nosenko, T. Shimizu, J. van Dijk, J. L. Zimmermann, *N. J. Phys.* **2009**, *11*(11), 115012. https://doi.org/10.1088/1367-2630/11/11/115012
[3] T. von Woedtke, S. Emmert, H.-R. Metelmann, S. Rupf, K.-D. Weltmann, *Phys. Plasmas* **2020** *27*(7), 070601. https://doi.org/10.1063/5.0008093
[4] S. Bekeschus, T. von Woedtke, S. Emmert, A. Schmidt, *Redox Biol.* **2021**, *46*, 102116. https://doi.org/10.1016/j.redox.2021.102116
[5] A. Soneja, M. Drews, T. Malinski, *Pharmacol. Rep.* **2005**, *57*(Suppl), 108.
[6] D. B. Graves, *J. Phys. D* **2012**, *45*(26), 263001. https://doi.org/10.1088/0022-3727/45/26/263001
[7] E. Carbone, C. Douat, *Plasma Med.* **2018**, *8*(1), 93. https://doi.org/10.1615/PlasmaMed.v8.i1
[8] B. E. Mann, R. Motterlini, *Chem. Commun.* **2007**, *102*, 4197. https://doi.org/10.1039/B704873D
[9] A. Fridman, *Plasma Chemistry*, Cambridge University Press, Cambridge **2008**.
[10] A. Bogaerts, T. Kozák, K. van Laer, R. Snoeckx, *Faraday Discuss.* **2015**, *183*, 217. https://doi.org/10.1039/C5FD00053J
[11] C. Douat, S. Ponduri, T. Boumans, O. Guaitella, S. Welzel, E. Carbone, R. Engeln, *Plasma Sources Sci. Technol.* **2023**, *32*(5), 055001. https://doi.org/10.1088/1361-6595/acceca
[12] G. Willems, A. Hecimovic, K. Sgonina, E. Carbone, J. Benedikt, *Plasma Phys. Control. Fusion* **2020**, *62*(3), 034005. https://doi.org/10.1088/1361-6587/ab6b4c
[13] C. Douat, P. Escot Bocanegra, S. Dozias, É. Robert, R. Motterlini, *Plasma Process. Polym.* **2021**, *18*(9), 2100069. https://doi.org/10.1002/ppap.v18.9
[14] T. Urbanietz, M. Böke, V. S. von der Gathen, A. von Keudell, *J. Phys. D* **2018**, *51*(34), 345202. https://doi.org/10.1088/1361-6463/aad4d3
[15] C. Stewig, S. Schü ttler, T. Urbanietz, M. Böke, A. von Keudell, *J. Phys. D* **2020**, *53*(12), 125205. https://doi.org/10.1088/1361-6463/ab634f
[16] J. Golda, J. Held, B. Redeker, M. Konkowski, P. Beijer, A. Sobota, G. Kroesen, N. S. J. Braithwaite, S. Reuter, M. M. Turner, D. O'Connell, V. Schulz-vonderGathen, *J. Phys. D* **2016**, *49*(8), 084003. https://doi.org/10.1088/0022-3727/49/8/084003
[17] R. Snoeckx, A. Bogaerts, *Chem. Soc. Rev.* **2017**, *46*, 5805. https://doi.org/10.1039/C6CS00066E
[18] T. Maho, R. Binois, F. Brulé-Morabito, M. Demasure, C. Douat, S. Dozias, P. Bocanegra, I. Goard, L. Hocqueloux, C. Helloco, I. Orel, J.-M. Pouvesle, T. Prazuck, A. Stancampiano, C. Tocaben, E. Robert, *Appl. Sci.* **2021**, *11*, 9598. https://doi.org/10.3390/app11209598
[19] M. Benčina, M. Resnik, P. Starič, I. Junkar, *Molecules* **2021**, *26*, 5. https://doi.org/10.3390/molecules26051418
[20] M. J. Nicol, T. R. Brubaker, B. J. Honish, A. N. Simmons, A. Kazemi, M. A. Geissel, C. T. Whalen, C. A. Siedlecki, S. G. Bilén, S. D. Knecht, G. S. Kirimanjeswara, *Scientific Rep.* **2020** *10*(1), 3066. https://doi.org/10.1038/s41598-020-59652-6

[21] G. Daeschlein, T. von Woedtke, E. Kindel, R. Brandenburg, K.-D. Weltmann, M. Jü nger, *Plasma Process. Polym.* **2010**, *7*(3–4), 224. https://doi.org/10.1002/ppap.200900059

[22] J. Louise Wilson, E. J. Helen, K. P. Robert, S. D. Kelly, *Curr. Pharm. Biotechnol.* **2012**, *13*, 760. https://doi.org/10.2174/138920112800399329

[23] J. Cheng, J. Hu, *ChemMedChem* **2021**, *16*(24), 3628. https://doi.org/10.1002/cmdc.v16.24

[24] M. Desmard, R. Foresti, D. Morin, M. Dagouassat, A. Berdeaux, E. Denamur, S. H. Crook, B. E. Mann, D. Scapens, P. Montravers, J. Boczkowski, R. Motterlini, *Antioxid. Redox Signal.* **2012**, *16*(2), 153. https://doi.org/10.1089/ars.2011.3959

[25] H. M. Southam, T. W. Smith, R. L. Lyon, C. Liao, C. R. Trevitt, L. A. Middlemiss, F. L. Cox, J. A. Chapman, S. F. El-Khamisy, M. Hippler, M. P. Williamson, P. J. Henderson, R. K. Poole, *Redox Biol.* **2018**, *18*, 114. https://doi.org/10.1016/j.redox.2018.06.008

[26] M. Hofmans, P. Viegas, van O. Rooij, B. Klarenaar, O. Guaitella, A. Bourdon, A. Sobota, *Plasma Sources Sci. Technol.* **2020**, *29*(3), 034003. https://doi.org/10.1088/1361-6595/ab6d49

[27] J.-P. Boeuf, L. L. Yang, L. C. Pitchford, *J. Phys. D* **2013**, *46*(1), 015201. https://doi.org/10.1088/0022-3727/46/1/015201

[28] P. Zhu, B. Li, Z. Duan, J. Ouyang, *J. Phys. D* **2018**, *51*(40), 405202. https://doi.org/10.1088/1361-6463/aadb12

[29] J. Golda, F. Kogelheide, P. Awakowicz, V. S. von der Gathen, *Plasma Sources Sci. Technol.* **2019**, *28*(9), 095023. https://doi.org/10.1088/1361-6595/ab393d

[30] M. Lieberman, A. Lichtenberg, *Principles of Plasma Discharges and Materials Processing*, Wiley-Interscience, New Jersey **2005**.

[31] V. E. Bening, V. Y. Korolev, *Theory Probab. Appl.* **2005**, *49*(3), 377. https://doi.org/10.1137/S0040585X97981159

[32] A. Hazra, *J. Thorac. Dis.* **2017**, *9*(10), 4124. https://doi.org/10.21037/jtd.2017.09.14

[33] U. Goebel, J. Wollborn, *Intensive Care Med. Exp.* **2020**, *8*, 2. https://doi.org/10.1186/s40635-020-0292-8

[34] R. Aerts, W. Somers, A. Bogaerts, *ChemSusChem* **2015**, *8*(4), 702. https://doi.org/10.1002/cssc.v8.4

[35] S. Ponduri, M. M. Becker, S. Welzel, M. C. M. van de Sanden, D. Loffhagen, R. Engeln, *J. Appl. Phys.* **2016**, *119*(9), 093301. https://doi.org/10.1063/1.4941530

[36] K. McKay, J.-S. Oh, J. L. Walsh, J. W. Bradley, *J. Phys. D* **2013**, *46*(46), 464018. https://doi.org/10.1088/0022-3727/46/46/464018

[37] T. Darny, J.-M. Pouvesle, J. Fontane, L. Joly, S. Dozias, E. Robert, *Plasma Sources Sci. Technol.* **2017**, *26*(10), 105001. https://doi.org/10.1088/1361-6595/aa8877

[38] M. Harden, A. He, K. Creamer, M. Clark, I. Hamdallah, K. Martinez 2nd, R. Kresslein, S. Bush, J. Slonczewski, *Appl. Environ. Microbiol.* **2015**, *81*, 1932. https://doi.org/10.1128/AEM.03494-14

[39] Y. Gao, K. Francis, X. Zhang, *Food Res. Int.* **2022**, *157*, 111246. https://doi.org/10.1016/j.foodres.2022.111246

[40] D. Boehm, P. Bourke, *Biol. Chem.* **2019**, *400*(1), 3. https://doi.org/10.1515/hsz-2018-0222

[41] T. von Woedtke, S. Reuter, K. Masur, K.-D. Weltmann, *Phys. Rep.* **2013**, *530*(4), 291. https://doi.org/10.1016/j.physrep.2013.05.005

[42] C. Douat, T. Dufour, J. S. Sousa, *Reflets Phys.* **2023**, *75*, 24. https://doi.org/10.1051/refdp/202375024

[43] J. L. R. Roti, *Int. J. Hyperthermia* **2008**, *24*(1), 3. https://doi.org/10.1080/02656730701769841

[44] E. Gayán, S. Monfort, I. Álvarez, S. Condón, *Innov. Food Sci. Emerg. Technol.* **2011**, *12*(4), 531. https://doi.org/10.1016/j.ifset.2011.07.008

[45] S. Kelly, J. Golda, M. M. Turner, V. S. von der Gathen, *J. Phys. D* **2015**, *48*(44), 444002. https://doi.org/10.1088/0022-3727/48/44/444002

[46] F. do Nascimento, T. Gerling, K. G. Kostov, *Phys. Scr.* **2023**, *98*(5), 055013. https://doi.org/10.1088/1402-4896/accb17

[47] A. V. Nastuta, T. Gerling, *Appl. Sci.* **2022**, *12*(2), 644. https://doi.org/10.3390/app12020644

[48] K. Lofty, *AIP Adv.* **2020**, *10*(1), 015303. https://doi.org/10.1063/1.5099923

[49] U. Cvelbar, D. Vujosevic, Z. Vratnica, M. Mozetic, *J. Phys. D* **2006**, *39*(16), 3487. https://doi.org/10.1088/0022-3727/39/16/S06

[50] D. Steuer, I. Korolov, S. Chur, J. Schulze, V. S. von der Gathen, J. Golda, M. Böke, *J. Phys. D* **2021**, *54*(35), 355204. https://doi.org/10.1088/1361-6463/ac09b9

[51] G. Willems, J. Golda, D. Ellerweg, J. Benedikt, A. von Keudell, N. Knake, V. S. von der Gathen, *New J. Phys.* **2019**, *21*(5), 059501. https://doi.org/10.1088/1367-2630/ab1dfc

[52] T. Murakami, K. Niemi, T. Gans, D. O'Connell, W. G. Graham, *Plasma Sources Sci. Technol.* **2012**, *22*(1), 015003. https://doi.org/10.1088/0963-0252/22/1/015003

[53] D. Ellerweg, A. von Keudell, J. Benedikt, *Plasma Sources Sci. Technol.* **2012**, *21*(3), 034019. https://doi.org/10.1088/0963-0252/21/3/034019

[54] J. D. McClurkin, D. E. Maier, in *Proceedings of the 10th International Working Conference on Stored Product Protection*, Vol. 425, Julius Kühn-Institut, Estoril, Portugal **2010**, pp. 381–385. https://doi.org/10.5073/jka.2010.425.167.326

[55] D. Ellerweg, J. Benedikt, A. von Keudell, N. Knake, V. S. von der Gathen, *New J. Phys.* **2010**, *12*(1), 013021. https://doi.org/10.1088/1367-2630/12/1/013021

[56] J. Jeong, J. Park, I. Henins, S. Babayan, V. Tú, G. Selwyn, G. Ding, R. Hicks, *J. Chem. Phys. A* **2000**, *104*, 8027. https://doi.org/10.1021/jp0012449

[57] M. J. Pavlovich, H.-W. Chang, Y. Sakiyama, D. S. Clark, D. B. Graves, *J. Phys. D* **2013**, *46*(14), 145202. https://doi.org/10.1088/0022-3727/46/14/145202

[58] A. Niveditha, R. Pandiselvam, V. A. Prasath, S. K. Singh, K. Gul, A. Kothakota, *Food Control* **2021**, *130*, 108338. https://doi.org/10.1016/j.foodcont.2021.108338

[59] N. Mastanaiah, P. Banerjee, J. A. Johnson, S. Roy, *Plasma Process. Polym.* **2013**, *10*(12), 1120. https://doi.org/10.1002/ppap.v10.12

[60] J. Waskoenig, K. Niemi, N. Knake, L. M. Graham, S. Reuter, V. S. von der Gathen, T. Gans, *Plasma Sources Sci. Technol.* **2010**, *19*(4), 045018. https://doi.org/10.1088/0963-0252/19/4/045018

[61] J. S. Sousa, K. Niemi, L. J. Cox, Q. T. Algwari, T. Gans, D. O'Connell, *J. Appl. Phys.* **2011**, *109*, 123302. https://doi.org/10.1063/1.3601347

[62] H. Wu, P. Sun, H. Feng, H. Zhou, R. Wang, Y. Liang, J. Lu, W. Zhu, J. Zhang, J. Fang, *Plasma Process. Polym.* **2012**, *9*(4), 417. https://doi.org/10.1002/ppap.v9.4

[63] J. Benedikt, D. Schröder, S. Schneider, G. Willems, A. Pajdarová, J. Vlček, V. S. von der Gathen, *Plasma Sources Sci. Technol.* **2016**, *25*(4), 045013. https://doi.org/10.1088/0963-0252/25/4/045013

[64] C. Douat, S. Huebner, R. Engeln, J. Benedikt, *Plasma Sources Sci. Technol.* **2016**, *25*(2), 025027. https://doi.org/10.1088/0963-0252/25/2/025027

[65] J. Golda, B. Biskup, V. Layes, T. Winzer, J. Benedikt, *Plasma Process. Polym.* **2020**, *17*(6), 1900216. https://doi.org/10.1002/ppap.v17.6

[66] S. Schneider, J.-W. Lackmann, D. Ellerweg, B. Denis, F. Narberhaus, J. E. Bandow, J. Benedikt, *Plasma Process. Polym.* **2012**, *9*(6), 561. https://doi.org/10.1002/ppap.v9.6

How to cite this article: E. Mestre, I. Orel, D. Henze, L. Chauvet, S. Burhenn, S. Dozias, F. Brulé-Morabito, J. Golda, C. Douat, *Plasma. Process. Polym.* **2023**, e2300182. https://doi.org/10.1002/ppap.202300182